

See discussions, stats, and author profiles for this publication at: <https://www.researchgate.net/publication/231634502>

Direct Observation of Solvation Dynamics and Dielectric Relaxation in the Photosynthetic Light-Harvesting-2 Complex of *Rhodospseudomonas acidophila*

ARTICLE *in* THE JOURNAL OF PHYSICAL CHEMISTRY B · FEBRUARY 2003

Impact Factor: 3.3 · DOI: 10.1021/jp026726u · Source: OAI

CITATIONS

9

READS

23

5 AUTHORS, INCLUDING:



[Frank van Mourik](#)

École Polytechnique Fédérale de Lausanne

121 PUBLICATIONS 3,569 CITATIONS

SEE PROFILE



[Raoul N Frese](#)

VU University Amsterdam

49 PUBLICATIONS 1,430 CITATIONS

SEE PROFILE



[Gert Van der Zwan](#)

VU University Amsterdam

107 PUBLICATIONS 2,665 CITATIONS

SEE PROFILE



[Rienk van Grondelle](#)

VU University Amsterdam

647 PUBLICATIONS 23,687 CITATIONS

SEE PROFILE

Direct Observation of Solvation Dynamics and Dielectric Relaxation in the Photosynthetic Light-Harvesting-2 Complex of *Rhodospseudomonas acidophila*

Frank van Mourik,^{*,†} Raoul N. Frese,[‡] Gert van der Zwan,[§] Richard J. Cogdell,^{||} and Rienk van Grondelle[‡]

Department of Biophysics and Physics of Complex Systems, Faculty of Sciences, Vrije Universiteit, De Boelelaan 1081, 1081HV Amsterdam, The Netherlands, Institut de Physique de la Matière Condensée, Faculté des Sciences, Université de Lausanne, CH-1015 Lausanne-Dorigny, Switzerland, Department of Analytical Chemistry and Applied Spectroscopy, Faculty of Sciences, Vrije Universiteit, De Boelelaan 1083, 1081HV Amsterdam, The Netherlands, and Division of Biochemistry and Molecular Biology, Institute of Biomedical and Life Sciences, University of Glasgow, G12 8QQ Glasgow, United Kingdom

Received: August 9, 2002; In Final Form: December 21, 2002

We studied the fluorescence dynamics of the light-harvesting-2 complex of *Rhodospseudomonas acidophila* both with and without an externally applied electric field. The fluorescence emission spectrum of the complex shows (small) spectral shifts of the average emission wavelength on a time scale of ~ 300 ps. The shifts are temperature dependent and result from a combination of the (a) dielectric relaxation, or solvation, of the excited states by the protein, which causes a red shift of the emission, and (b) nonradiative loss processes occurring in a subset of the ensemble of complexes. These two processes compete with delocalization and energy transfer around the ring and are shown to be sensitive to an external electric field. The experiments illustrate how nature has prevented the above-mentioned loss processes in vivo by having fast energy transfer around a symmetric structure. Local protein relaxation is slow for the delocalized (or fast-hopping) excited states. However, once localized, localization and (dielectric) relaxation act in a cooperative way. Therefore, at low temperatures (< 100 K), the nonradiative loss processes are more prominent. In a more general way, the experiments demonstrate how, by looking at the effects of an external electric field on the fluorescence dynamics, one can identify the nature of the relaxation processes; that is, the electric field is a probe for solvation and relaxation processes. These first experiments demonstrate the promising potential of the approach presented here for studies on ultrafast solvation processes.

Introduction

Light-Harvesting Complex. Light-harvesting complexes in photosynthetic systems are designed for fast energy transfer among the complexes and funneling of excitation energy to the reaction centers, where the primary charge separation takes place.¹ In the case of the photosynthetic purple bacteria, the light-harvesting complexes all come in the form of rings of pigment molecules bound to short trans-membrane polypeptides.^{2,3} The so-called light-harvesting-2 (LH2) complexes consist of two rings of pigments, the B800 ring and the B850 ring, named after their near-IR absorption maxima. Here we are only interested in the B850 ring, containing 18 (or 16)³ bacteriochlorophyll molecules, because of its intriguing spectroscopic and electrooptic properties. For our experiments, we actually chose to use a blue-shifted variety of LH2, sometimes called LH3, for practical reasons; its emission spectrum is much better suited for detection with our Streak camera. Apart from a blue shift, the B850 (B820) band of this complex has structural,⁴ spectroscopic,⁵ and electrooptic properties^{6,7} similar

to those of the B850 band of the well-characterized LH2 complexes. In the following, we will refer to it as B850, even though its absorption maximum peaks at ~ 820 nm. The pigment molecules in the B850 ring are very densely packed, with a center-to-center distance between nearest neighbors of less than 1 nm. The coupling between the pigments has a strong effect on the spectroscopy of the complex. A large number of experimental and theoretical studies have appeared on the spectroscopic properties of LH2, mostly focusing on the degree of delocalization of the excited states of the B850 ring.^{8–12} The actual degree of delocalization depends on the ratio between the energetic disorder over the ring (imposed by the protein) and the electronic coupling between the pigments. Experimental work generally indicates an intermediate case for B850, but there is still a lack of agreement on the actual coupling strength and disorder parameters, and the outcome depends on the inherent time scale of the experiment. When studying the fluorescence superradiance, one typically finds delocalization over 3–4 pigments.⁸ Apparently, the (sub)picosecond relaxation processes observed in femtosecond nonlinear experiments^{13–16} reduce the degree of delocalization on the picosecond time scale probed in fluorescence experiments. On the other hand, it should be noted that even at low temperature the excited states are still very mobile; for example, singlet–singlet annihilation experiments are indicative of diffusive motion over large distances in the light-harvesting network.¹⁷

* Corresponding author. E-mail: Frank.vanMourik@ipmc.unil.ch.

[†] Université de Lausanne.

[‡] Department of Biophysics and Physics of Complex Systems, Vrije Universiteit.

[§] Department of Analytical Chemistry and Applied Spectroscopy, Vrije Universiteit.

^{||} University of Glasgow.

The aim of the experiments presented here is twofold. First of all, we want to get a better idea of the nature of the B850 excited state on the time scales relevant for its light-harvesting function. Second, this is a new type of experiment which allows one to time-resolve the dielectric response of a protein,^{24,25} which plays a central role in the theory of (biological) electron-transfer processes.^{18,19}

Materials and Methods

Sample Treatment. The LH2 (LH3) complexes from *R. acidophila* were diluted with a 60% w/v glycerol buffer (10 mM Tris-HCl, pH 8.0, 0.1% LDAO) to obtain a good glass. Stark measurements were performed in a 0.1-mm-path-length Stark cell.^{20,21} The cell was emerged in liquid nitrogen in an Oxford cryostat.

Absorption, Fluorescence, and Stark Spectroscopy. The measurements were performed on an integrated setup for steady-state absorption and fluorescence, Stark absorption and Stark fluorescence, and time-resolved Stark fluorescence measurements. The steady-state fluorescence measurements were performed by exciting the sample with light from a tungsten lamp passing through a 514-nm interference filter and detected at 90° through a monochromator (bandwidth ~10 nm) with a photodiode. All fluorescence experiments were performed by excitation around 514 nm, because at this wavelength the Stark absorption signal is zero. The setup and technique for the steady-state Stark measurements are described elsewhere.⁷ The line shape of the steady-state Stark absorption spectrum is modeled by fitting the absorption spectrum to a polynomial function (splines) and the Stark spectrum with the zeroth, first, and second derivative of this function as described in ref 22. Typical values for the applied electric field are 1 MV/cm.

Time-Resolved Stark Fluorescence Spectroscopy. The time-resolved Stark fluorescence setup is a combination of a time-resolved fluorescence setup with a Synchroscan Streak camera as the detector and an amplified Ti:sapphire laser system as the excitation source. The Streak camera has two sets of perpendicular electron deflection plates; as usual, the vertical deflection plates are swept synchronous to the Ti:sapphire oscillator. The horizontal plates were connected to the High Voltage sine-wave generator, which also generates the electric field applied over the sample. Therefore, the horizontal position of the two-dimensional output of the Streak camera corresponds with the electric field at the sample and the vertical position with the time of arrival of the fluorescence photon. The field over the sample could be switched off independently so that the two-dimensional images could be recorded with and without a Stark field to calculate a difference signal. Note that the fluorescence lifetime of LH2 is ~2 ns, whereas the electric-field sweep is modulated with 310 Hz. Therefore, the electric field can be regarded as constant on the time scale of the fluorescence.

Excitation pulses of ~150 fs at 514 nm were generated at a ~50-kHz repetition rate using a Ti:sapphire oscillator (Coherent MIRA SEED), a regenerative amplifier (Coherent REGA), and a double-pass optical parametric amplifier (Coherent OPA-9400). The fluorescence was measured through band-pass or RG830 colored glass filters. Detection was at a right angle to the excitation, and the emission was focused on the center of the entrance slit of a Hamamatsu C5680 Synchroscan Streak camera with an S25 photocathode. The Streak images were recorded on a Hamamatsu C4880 CCD camera, which was cooled to -55 °C. The full width at half-maximum of the instrumental time response was 3 ps.²³

Time-Resolved Fluorescence Spectra. Time-resolved fluorescence measurements were recorded with a Streak camera as described elsewhere²³ with the same setup as the time-resolved Stark fluorescence measurements, but now the fluorescence is detected through a spectrograph (Chromex 250IS), which images the emission spectrum onto the horizontal slit of the Streak camera. The 77 and 230 K data were measured on the same sample with a maximum optical density of 0.06 in 1-cm cuvettes. The typical power used on the sample was 180 μW at a pulse repetition rate of 40 kHz. The fluorescence spectra were measured with vertically polarized excitation and magic angle detection.

Results

In this work, we try for the first time to use Stark spectroscopy to time-resolve dielectric relaxation processes in a protein on a picosecond time scale. As a probe for the local electric field in the protein, we use the excited state of B850. The electrooptic properties of the B850 rings are largely due to the above-mentioned excitonic nature of the transitions. Stark absorption experiments indicate rather small changes in the dipole moment and a very large increase in polarizability when going from the ground to the excited state.^{6,7} Both observations are not surprising; a centrosymmetric supermolecule a priori has no permanent dipole moment in its ground and excited states; therefore, any dipole moment must be induced by symmetry breaking. The very high polarizability of the excited state is probably due to the large number of transitions from the 1-exciton band to the 2-exciton band²⁶ and intraband transitions.²⁷ Note that this high polarizability of the excited state is not a desired design parameter for a light-harvesting complex because it makes the excited state very sensitive to fluctuations in the local electric field. As we will see, this can lead to loss processes.

Stark Spectroscopy. An electronic transition in a molecule perturbed by a local electric field will be shifted in frequency as given in formula 1. Here, $\Delta\vec{\mu}$ is the difference in the dipole

$$\Delta\nu = -\frac{1}{h}(\vec{E} \cdot \Delta\vec{\mu} + \frac{1}{2}\vec{E} \cdot \Delta\vec{\alpha} \cdot \vec{E}) \quad (1)$$

moment between the excited and ground states, and $\Delta\vec{\alpha}$ is the difference between the polarizability tensors of the excited and ground states. In a Stark experiment, the local field around the molecule of interest is the sum of the internal field produced by the protein and the externally applied field

$$\vec{E} = \vec{E}_{\text{int}} + f\vec{E}_{\text{ext}} \quad (2)$$

Here, f represents the correction for the fact that the pigment molecule is in a cavity within the protein. The value of f depends on the cavity dimensions and the dielectric properties of the protein; generally values of 1.2–1.4 are used or assumed.²¹ The internal field in a polar medium is typically a few orders of magnitude stronger than the externally applied field. Field strengths on the order of tens of megavolts per centimeter have been reported for the binding pocket inside Myoglobin.^{28,29} We have recently shown that the asymmetric line shape of the B800 band of LH2 can be very well described by presuming a Gaussian distribution for \vec{E}_{int} .³⁰ For the experiments described below, it is important that \vec{E}_{int} is not a static quantity. It contains the reaction field of the protein, that is, the dielectric response of the protein to the change in the charge distribution in the chromophore upon going from the ground to the excited state.

Combining formulas 1 and 2 gives formula 3.

$$\Delta\nu = -\frac{1}{\hbar}(\vec{E}_{\text{int}} \cdot \Delta\vec{\mu} + \frac{1}{2}\vec{E}_{\text{int}} \cdot \Delta\vec{\alpha} \cdot \vec{E}_{\text{int}} \quad (3a)$$

$$+ f \cdot \vec{E}_{\text{ext}} \cdot \Delta\vec{\mu} + \frac{1}{2}f^2 \cdot \vec{E}_{\text{ext}} \cdot \Delta\vec{\alpha} \cdot \vec{E}_{\text{ext}} \quad (3b)$$

$$+ \frac{1}{2}f \cdot \vec{E}_{\text{ext}} \cdot \Delta\vec{\alpha} \cdot \vec{E}_{\text{int}}) \quad (3c)$$

Here, the first two terms represent the solvent shift and inhomogeneous broadening of the transition resulting from the protein field. These terms obviously do not depend on the external field. The rest of the terms represent the Stark effect. However, note that the last term is generally not mentioned as such because it normally cannot be distinguished from the dipolar term in formula 3b. What is important here is that \vec{E}_{int} also comprises the reaction field of the protein. Therefore, in a time-resolved (excited-state) Stark experiment the last term, in principle, allows one to single out the time dependence of the reaction field as the only time-dependent quantity that is sensitive to the external field.

Deviations Due to Energy Transfer. For analyzing Stark absorption experiments, the formalism of Liptay³¹ is generally used to extract the intrinsic molecular parameters from the spectral shifts and broadening in an electric field. This approach also works for Stark fluorescence.⁶ However, as outlined below, it is not valid once the (Stark) fluorescence of a set of coupled chromophores, among which energy transfer occurs, is studied. Therefore, we start here with a numerical evaluation of this effect. Consider a ring of identical chromophores that are weakly coupled and that each have a difference dipole moment. If we apply an electric field over the ring, each of the chromophores will have a different orientation with respect to the field. Therefore, the energy shifts of the excited states of the chromophores will be different. If we now presume efficient energy transfer between the chromophores, the electric field will perturb the Boltzmann distribution of the excited states over the ring. For energy shifts that are on the order of $k_B T$, this means that mostly the chromophores that have a red shift resulting from the field will be populated in the “equilibrated excited state”. Therefore, the interaction of the field with the difference dipole moments will not broaden the emission spectrum; rather, it will cause a red shift of the emission. We evaluated this effect numerically for different numbers of chromophores (pigments or clusters) per ring, with inhomogeneously broadened site energies, as a function of temperature. Because the effect depends on the particular realization of the site energies, the calculation was performed over a large set of rings with Gaussian-distributed site energies. The goal is to calculate the shifts and broadening of the excited-state population resulting from the electric field. To understand the results, it is useful to first consider the effects of temperature, inhomogeneous broadening, and ring size on the width and position of the excited-state population. Figure 1a shows the equilibrium width and shift of the excited-state population for a number of ring sizes. Obviously, increasing the number of coupled chromophores at low temperatures leads to a shift to lower energies and a narrowing of the distribution, because then only the lowest-energy site of the ring will be populated. For the case of two chromophores, the average population shifts by $\sigma/\sqrt{\pi}$ for $T = 0$.

Figure 1b shows the effect of an electric field on the distributions in Figure 1a. One simplistic way of looking at this

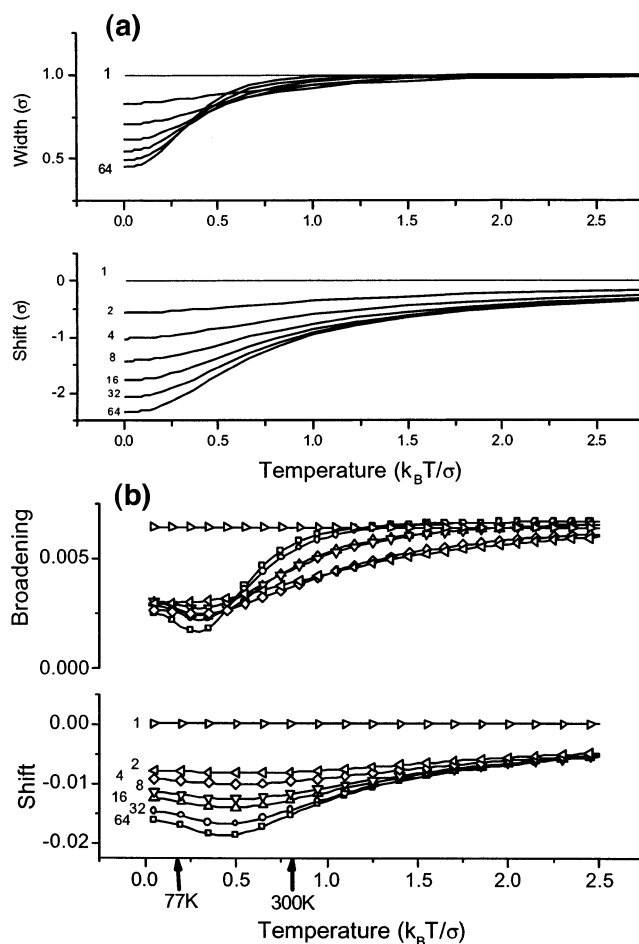


Figure 1. (a) Numerical calculations of the width and position of the equilibrium excited-state population of clusters of inhomogeneously broadened pigments as a function of temperature. The cluster sizes were 1, 2, 4, 8, 16, 32, and 64. The shifts, widths, and temperatures are scaled to the width(s) of the Gaussian inhomogeneous distribution. (b) Numerical calculation of the effect of an electric field on the curves of part a. The upper panel shows the electric-field-induced increase in the width of the excited-state distribution. The broadening and shift values are both expressed in the same units as those of σ . The lower panel shows the red shift. The site inhomogeneity was chosen to be $\sigma = 250 \text{ cm}^{-1}$, the difference dipole moments of each of the sites $\Delta\mu = 3 \text{ D}$, and the electric field $E = 1 \text{ MV/cm}$. The arrows indicate the positions on the scale of 300 K and 77 K for the chosen value of σ .

is that the electric field increases the inhomogeneous width; that is, it causes a shift to lower effective temperature in Figure 1a. However, because the effects on the different chromophores along the ring are correlated on the basis of their fixed relative geometry, this is not strictly correct. Therefore, we calculated the perturbation by the electric field numerically and took the average over all the possible orientations of the rings with respect to the electric field. In the calculations, a difference dipole moment of 3 D was used, in combination with an electric field of 1 MV/cm. No photoselection effects were taken into account. The difference dipole moments were taken to be oriented in the plane of the ring and tangential to the ring. This configuration was chosen to mimic the B850 ring. However, the calculations are not limited to this geometry; all geometries in which there is a variation of the interaction of the dipole moments with the electric field will show the described effect. Figure 1b shows the calculated change in the position and width of the excited-state population induced by the electric field. The temperature scale is normalized to the width of the inhomogeneous distribution. The arrows indicate the position of room

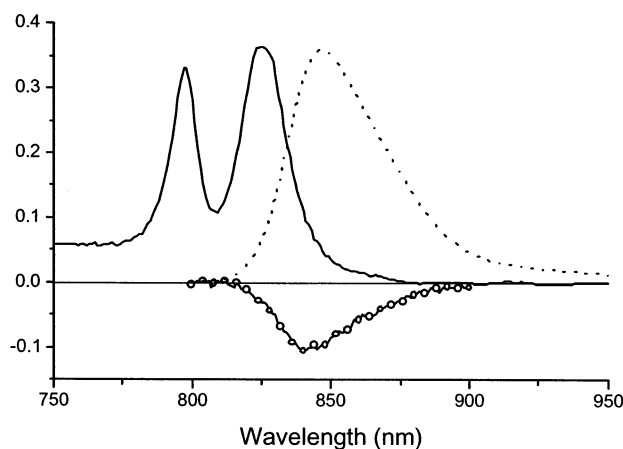


Figure 2. 77 K absorption (solid), fluorescence (dashed), and Stark fluorescence difference (circles) spectra of the B800–B820 LH2 complexes from *R. acidophila*. All spectra were recorded in the Stark cell, and the electric field in the Stark fluorescence experiment was 0.6 MV/cm. The Stark fluorescence is shown as the difference in fluorescence with the field off minus that with the field on. The change in fluorescence resulting from the electric field corresponds with a loss of 3% relative to the zero-field spectrum.

temperature and 77 K on the scale for a choice of $\sigma = 250 \text{ cm}^{-1}$ for the width of the inhomogeneous distribution.³²

The curves in Figure 1b clearly demonstrate that, whereas normally the coupling between (difference) dipole moments and an electric field results in the broadening of a transition, the emission from a ring of coupled chromophores will mostly show a red shift of the emission. The result also does not depend too strongly on a choice for the number of clusters; as long as the ring is broken up into two or more clusters, the electric-field-induced broadening diminishes and is replaced by a field-induced red shift. Therefore, our treatment is independent of assumptions on the degree of delocalization of the excited state.

All the results scale with the square of the electric field. For the broadening, this is not surprising because this is similar to the case of monomeric pigments with a difference dipole moment. The lines corresponding with a single chromophore of course correspond with this case (no shift, only broadening). The square-law dependence of the red shift can be understood by analogy with the polarizability of a molecule. The electric field affects the distribution of the excited states, and with them the excited-state dipole moments, over the ring. Therefore, the electric field interacts with an induced dipole moment, hence the square dependence on the field. What is special here is that this “ring polarizability” is temperature dependent.

The 77 K absorption and steady-state fluorescence emission spectra of the LH2 complex are shown in Figure 2. The absorption spectrum shows the two bands characteristic for this LH2 complex. The B800 band peaks at 800 nm, and the B850 band peaks at 824 nm. The maximum of the fluorescence is at 846 nm. Note that the fluorescence line shape is significantly broader than that of the absorption profile (see Discussion).

The 77 K Stark fluorescence spectrum (fluorescence with field minus fluorescence without field) is very similar in shape to the published Stark fluorescence spectrum of LH2 from *Rhodobacter sphaeroides*.⁶ The minimum of the Stark fluorescence spectrum is blue-shifted 6 nm with respect to the fluorescence maximum (that is, 840 and 846 nm). The decrease of the Stark fluorescence is 3% of the fluorescence without field. This is about a factor of 2 higher than what was found for LH2 from *Rb. sphaeroides*.^{6,7} The shape of the difference emission spectrum is anomalous.⁶ On the basis of the large difference in

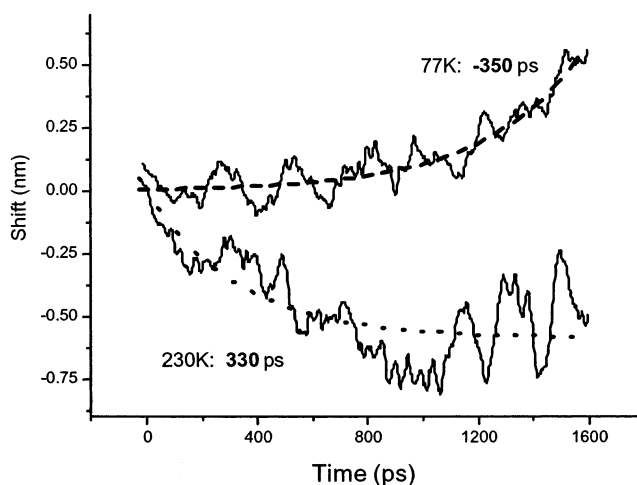


Figure 3. Time dependence of the first moment of the LH2 fluorescence emission spectrum. The measurements were performed at 77 and 230 K. A positive value corresponds with a blue shift of the average emission. The dashed lines are fits of the data with exponential lifetimes of 330 (230 K) and –350 ps (77 K).

polarizability (obtained from the Stark absorption spectrum), we would have expected a strong band shift, that is, a first derivative signal for the difference emission spectrum. However, the difference spectrum cannot be described as a combination of the derivatives of the emission line shape. It can be described as a combination of a first derivative plus a field-induced loss process (loss of dipole strength, or quenching) occurring mostly in the red part of the spectrum.

We also checked the 77 K Stark absorption (results not shown) of the samples used in the following (Stark) fluorescence experiments. Treating the B850 band as arising from one single band, we obtain a good fit of the Stark spectrum using a large first-derivative component, a moderate second-derivative component, and some negative zeroth-derivative contribution. The parameters obtained from the fit are $\Delta\bar{\mu} = 3.3 \text{ D/f}$ and $\Delta\alpha = 1400 \text{ \AA}^3/f^2$, which is similar to what was reported before.⁷ Compared to the LH2 complex of *Rb. sphaeroides*, the permanent dipole moments are similar but the value for the difference polarizability of the B850 pigments is 2 times higher.

Time-Resolved Fluorescence at 77 and 230 K. Figure 3 shows the time dependence of the average emission wavelength of the emission spectrum at 230 and 77 K. The spectral changes observed in the time-resolved emission spectra are rather small; therefore, we show the first moment of the emission spectrum as a function of time. Note that the curves obtained at these two temperatures *could hardly be more different*. First of all, the direction of the shift is different for the two temperatures, but what is more striking is the time behavior of the 77 K trace. The 230 K emission shows a more or less exponential red shift, which is what one would expect for a relaxation process in the excited state.³³ The curve for the 77 K emission corresponds with a blue shift. The time-resolved spectra (not shown here) reveal that this is not due to an overall shift to the blue of the emission spectrum as a function of time. Instead, there is a loss of fluorescence in the red wing of the spectrum that is responsible for the blue shift of the average. The very peculiar time dependence (here fitted with a rising exponential) of the shift at 77 K is typical for cooperative processes (see Discussion).³⁴

Time-Resolved Stark Fluorescence. Figure 4 shows the effect of an electric field on the intensity of the fluorescence (integrated over the spectrum) as a function of time, measured

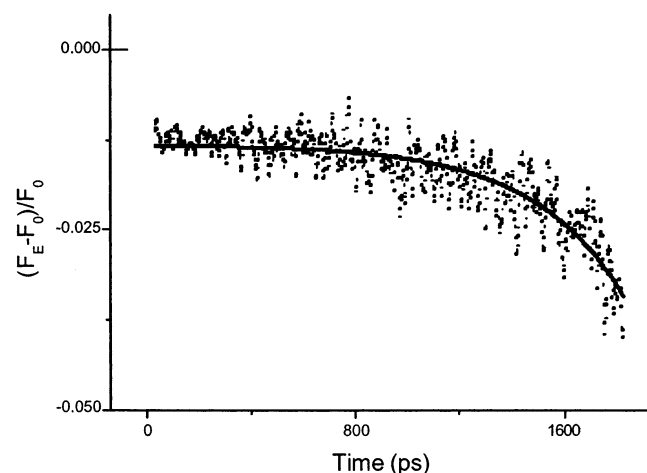


Figure 4. Time-resolved Stark fluorescence yield depicted as the difference in the fluorescence yield with the field on minus that with the field off weighted by the yield without field. The measurements were performed at 77 K. The dots are calculated from single time slices, and the curve through the points is a fit using a fixed lifetime of ~ 350 ps (as in Figure 3).

at 77 K. At short times, there is a difference of about 1% between the emission with and without the Stark field. This difference is more or less constant in the first 50 ps. At longer times, the field sensitivity increases. Clearly, the time dependence of the field sensitivity resembles the 77 K curve of Figure 3, and the curve drawn through the points is a fit with the same lifetime as that in Figure 3. The strong increase in field sensitivity in part explains the discrepancy between the magnitude of the Stark absorption and Stark fluorescence experiments noted before.⁶ The nature of the excited state changes during the excited-state lifetime. We also measured the Stark fluorescence signal with the highest available resolution of our Streak camera (~ 2 ps) but found no changes in the first tens of picoseconds.

Discussion

It is important to note here again that the magnitudes of the observed spectral shifts are very small. This is in strong contrast to what was reported by Polivka et al.,³⁵ where large spectral changes were reported on a picosecond to nanosecond time scale. This discrepancy is probably due to the different types of samples used. Here, we used solubilized complexes and great care was taken to avoid aggregation. Polivka et al. used membranes of LH2-only mutants. When we performed the time-resolved fluorescence experiments with lower detergent concentrations, so as to obtain aggregates, we indeed observed much larger spectral shifts on a time scale of tens of picoseconds. We think this shift is purely due to the equilibration among a large number of rings; time-resolved Stark experiments on this type of preparation would resolve this issue.

The steady-state fluorescence emission spectrum (77 K) gives an important clue about the nature of the excited state on a picosecond time scale. The emission spectrum is much broader than the absorption spectrum. This is not special for the complex we are studying here; it is observed in all LH2 complexes. If we would try to understand this within the exciton model, we would run into a problem because the emission at 77 K is mostly from the lowest excited state, and the emission should, in fact, be narrower than that in the absorption spectrum.

We think that the most likely explanation for the broadening of the emission comes from the very high polarizability of the excited state. As a consequence of this high polarizability,

relaxation of the excited state should actually result in more dipole character. This corresponds with an increase in the horizontal displacement (on the nuclear–solvation coordinate) of the minimum of the excited-state potential curve relative to that of the ground-state potential. Moreover, the excited-state potential will become more curved³⁶ in its minimum as a result of the increased interaction with the solvent fluctuations. Both these changes will increase the broadening of the emission spectrum. Moreover, the increased coupling of the dipole moment with the “solvent fluctuations” will have its effect on the delocalization length of the excited states; that is, the excited state will become more delocalized. This explains why the nature of the “relaxed” excited state is different from the state that is probed in the ground-state absorption spectrum. Note that it is not trivial to quantify this effect: the high polarizability is due to the exciton nature of the excited-state; therefore, reducing the degree of delocalization in turn decreases the polarizability!

The time resolution of our fluorescence experiments is about 2 ps. In our experiments, we do not see any dynamics occurring in the first tens of picoseconds; we have to presume that the change occurs on a subpicosecond time scale. Therefore, it looks like the superradiance and delocalization parameters derived from the steady-state emission⁸ are already valid after 1–2 ps. This is in line with most femtosecond experiments,^{14,15} which show that most of the “decoherence” occurs on a subpicosecond time scale. The time-resolved fluorescence anisotropy and annihilation experiments^{13,17} indicate that the excited states “hop” around the ring(s) on a (sub)picosecond time scale. This is important for the relaxation processes on a longer time scale; it will slow the development of local reaction fields in the protein. Interactions between the excited state and the protein fields are mostly short range (dipole–dipole or dipole–induced-dipole). Therefore, an excited state that hops around a ring only interacts with a certain site during short intervals of time. At normal temperatures, this appears to be sufficient to prevent dielectric relaxation on the time scale of light harvesting.

At low temperatures, the picture is slightly different; the energy transfer occurs on more or less the same time scale,^{37,38} but disorder causes an unequal average distribution of the excited state over the ring. If a site on the ring is slightly red shifted, this site will be preferentially populated at low temperatures. This is an unstable situation because the population of the site causes further protein relaxation at this site, lowering the energy of the site even more. This, in turn, will cause further localization and trapping on this site; that is, localization and relaxation are cooperative processes. The cooperative effects can be readily appreciated in Figures 3 and 4. This cooperative picture is reminiscent of the model described in ref 34.

To explain the observations, we have to presume that the final result of relaxation on a local site corresponds with a dark state, most probably a polaron or a charge-transfer state. The mechanism described above starts off with a red-shifted site on the ring, a site that is at least $\sim k_B T$ lower in energy than the other sites on the ring. This will not occur in all rings; only a small fraction of the ensemble of rings will have a site like that. This explains why the loss process mostly occurs in the red wing of the emission spectrum: the subset from the ensemble of rings that contains a sufficiently red-shifted site will (on the average) have a red-shifted emission spectrum relative to the emission spectrum averaged over the ensemble. The transformation into a dark state is not a gradual process because we do not observe any red-shifted intermediate state, which limits the lifetime of intermediates to $\lesssim 50$ ps. Therefore,

we think that, beyond a certain threshold, dielectric relaxation results in a charge-transfer state.

For the in vivo function of the LH2 complex, the loss processes unveiled here are probably of no importance. At physiological temperatures, the energy-transfer processes are fast enough to prevent localization and relaxation. Transfer between different complexes within the antenna occurs on a time scale of about 10 ps. The 230 K data of Figure 3 gives no indication for the "dielectric breakdown" observed at 77 K. We think this is mostly thanks to the symmetry of the complexes, which spreads the "load" of the excited state over the whole ring. Note that even at 77 K the "breakdown" only occurs in complexes that had a broken symmetry: a red-shifted site.

The time-resolved Stark fluorescence experiment nicely shows the potential of following the development of a reaction field (solvation of an excited state) using time-resolved Stark fluorescence. Unfortunately, the system at hand is too complicated to be described quantitatively with simple formulas. However, the combination of time-resolved fluorescence and Stark fluorescence makes it possible to unambiguously assign all field-sensitive dynamics to dielectric relaxation processes, that is, the formation of a reaction field.

Acknowledgment. The authors thank Drs. B. Gobets and J. A. Ihalainen for their contributions to the experiments. R.J.C. was supported by the Biotechnology and Biological Sciences Research Council.

References and Notes

- (1) Van Grondelle, R.; Dekker, J. P.; Gillbro, T.; Sundstrom, V. *Biochim. Biophys. Acta* **1994**, *1187* (1), 1–65.
- (2) Freer, A. A.; Prince, S. M.; Sauer, K.; Papiz, M. Z.; Hawthornwaite-Lawless, A. M.; McDermott, G.; Cogdell, R. J.; Isaacs, N. W. *Structure* **1996**, *4*, 449–462.
- (3) Koepke, J.; Hu, X.; Münke, C.; Schulten, K.; Michel, H. *Structure* **1996**, *4*, 581–597.
- (4) McLuskey, K.; Prince, S. M.; Cogdell, R. J.; Isaacs, N. W. *Biochemistry* **2001**, *40* (30), 8783–8789.
- (5) Fowler, G. J. S.; Visschers, R. W.; Grief, G. G.; van Grondelle, R.; Hunter, C. N. *Nature (London)* **1992**, *355*, 848–850.
- (6) Gottfried, D. S.; Stocker, J. W.; Boxer, S. G. *Biochim. Biophys. Acta* **1991**, *1059*, 63–75.
- (7) Beekman, L. M. P.; Frese, R. N.; Fowler, G. J. S.; Picorel, R.; Cogdell, R. J.; van Stokkum, I. H. M.; Hunter, C. N.; van Grondelle, R. *J. Phys. Chem. B* **1997**, *101*, 7293–7301.
- (8) Monshouwer, R.; Abrahamsson, M.; van Mourik, F.; van Grondelle, R. *J. Phys. Chem. B* **1997**, *101*, 7241–7248.
- (9) Meier, T.; Zhao, Y.; Chernyak, V.; Mukamel, S. *J. Chem. Phys.* **1997**, *107*, 3876–3893.
- (10) Bakalis, L. D.; Knoester, J. *J. Phys. Chem. B* **1999**, *103*, 6620–6628.
- (11) Nagarajan, V.; Alden, R. G.; Williams, J. C.; Parson, W. W. *Proc. Natl. Acad. Sci. U.S.A.* **1996**, *93*, 13774–13779.
- (12) Alden, R. G.; Johnson, E.; Nagarajan, V.; Parson, W. W.; Law, C. J.; Cogdell, R. G. *J. Phys. Chem. B* **1997**, *101*, 4667–4680.
- (13) Bradforth, S. E.; Jimenez, R.; van Mourik, F.; van Grondelle, R.; Fleming, G. R. *J. Phys. Chem.* **1995**, *99*, 16179–16191.
- (14) Jimenez, R.; van Mourik, F. Yu, J.-Y.; Fleming, G. R. *J. Phys. Chem. B* **1997**, *101*, 7350–7359.
- (15) Kumble, R.; Palese, S.; Visschers, R. W.; Dutton, P. L.; Hochstrasser, R. M. *Chem. Phys. Lett.* **1996**, *261* (4–5), 396–404.
- (16) Yang, M.; Fleming, G. R. *J. Chem. Phys.* **2000**, *113* (7), 2823–2840.
- (17) Vos, M.; van Grondelle, R.; van der Kooij, F. W.; van der Poll, D.; Ames, J.; Duysens, L. N. M. *Biochim. Biophys. Acta* **1986**, *850* (3), 501–512.
- (18) Sumi, H.; Marcus, R. A. *J. Chem. Phys.* **1986**, *84*, 4272–4276.
- (19) Bixon, M.; Jortner, J. *Chem. Phys.* **1993**, *176* (2–3), 467–481.
- (20) Boxer, S. G. In *Biophysical Techniques in Photosynthesis*; Ames, J., Hoff, A. J., Eds.; Kluwer Academic Publishers: Dordrecht, The Netherlands, 1996; pp 177–189.
- (21) Bublitz, G. U.; Boxer, S. G. *Annu. Rev. Phys. Chem.* **1997**, *48*, 213–242.
- (22) Frese, R.; Oberheide, U.; van Stokkum, I.; van Grondelle, R.; Foidl, M.; Oelze, J.; van Amerongen, H. *Photosynth. Res.* **1997**, *54*, 115–126.
- (23) Gobets, B.; van Stokkum, I. H. M.; Rogner, M.; Kruip, J.; Schlodder, E.; Karapetyan, N. V.; Dekker, J. P.; van Grondelle, R. *Biophys. J.* **2001**, *81* (1), 407–424.
- (24) Pierce, D. W.; Boxer, S. G. *J. Phys. Chem.* **1992**, *96*, 5560–5566.
- (25) Changelnet-Barret, P.; Choma, C. T.; Gooding, E. F.; DeGrado, W. F.; Hochstrasser, R. M. *J. Phys. Chem. B* **2000**, *104*, 9322–9329.
- (26) Somsen, O. J. G.; Chernyak, V.; Frese, R. N.; van Grondelle, R.; Mukamel, S. *J. Phys. Chem. B* **1998**, *102*, 8893–8908.
- (27) Kumble, R.; Howard, T. D.; Cogdell, R. J.; Hochstrasser, R. M. *J. Photochem. Photobiol., A* **2001**, *142*, 121–126.
- (28) Phillips, G. N.; Teodoro, M. L.; Li, T.; Smith, B.; Olson, J. S. *J. Phys. Chem. B* **1999**, *103*, 8817–8829.
- (29) Park, E. S.; Andrews, S. S.; Hu, R. B.; Boxer, S. G. *J. Phys. Chem. B* **1999**, *103* (45), 9813–9817.
- (30) van Mourik, F.; Chergui, M.; van der Zwan, G. *J. Phys. Chem. B* **2001**, *105*, 9715–9718.
- (31) Liptay, W. Dipole moments and polarizabilities of molecules in excited states. In *Excited States*; Lim, E. C., Ed.; Academic Press: New York, 1974; Vol. 1, 129–229.
- (32) Wendling, M.; Lapouge, K.; van Mourik, F.; Novoderezhkin, V.; Robert, B.; van Grondelle, R. *Chem. Phys.* **2002**, *275*, 31–45.
- (33) van der Zwan, G.; Hynes, J. T. *J. Phys. Chem.* **1985**, *89*, 4181–4188.
- (34) Christophorov, L. N.; Holzwarth, A. R.; Kharkyanen, V. N.; van Mourik, F. *Chem. Phys.* **2000**, *256*, 45–60.
- (35) Polivka, T.; Pullerits, T.; Herek, J. L.; Sundstrom, V. *J. Phys. Chem. B* **2000**, *104*, 1088–1096.
- (36) Carter, E. A.; Hynes, J. T. *J. Chem. Phys.* **1991**, *94*, 5961–5979.
- (37) Somsen, O. J. G.; van Mourik, F.; van Grondelle, R.; Valkunas, L. *Biophys. J.* **1994**, *66*, 1580–1596.
- (38) Visser, H. M.; Somsen, O. J. G.; van Mourik, F.; Lin, S.; van Stokkum, I. H. M.; van Grondelle, R. *Biophys. J.* **1995**, *69*, 1083–1099.